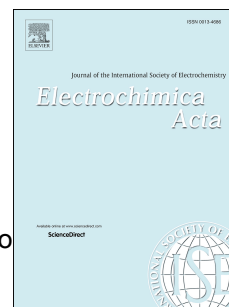


Journal Pre-proof

Electrochemical synthesis of fluorinated polyanilines

Nesrine Saidani, Emilia Morallón, Francisco Huerta, Salma Besbes-Hentati, Francisco Montilla



PII: S0013-4686(20)30721-0

DOI: <https://doi.org/10.1016/j.electacta.2020.136329>

Reference: EA 136329

To appear in: *Electrochimica Acta*

Received Date: 23 March 2020

Revised Date: 20 April 2020

Accepted Date: 25 April 2020

Please cite this article as: N. Saidani, E. Morallón, F. Huerta, S. Besbes-Hentati, F. Montilla, Electrochemical synthesis of fluorinated polyanilines, *Electrochimica Acta* (2020), doi: <https://doi.org/10.1016/j.electacta.2020.136329>.

This is a PDF file of an article that has undergone enhancements after acceptance, such as the addition of a cover page and metadata, and formatting for readability, but it is not yet the definitive version of record. This version will undergo additional copyediting, typesetting and review before it is published in its final form, but we are providing this version to give early visibility of the article. Please note that, during the production process, errors may be discovered which could affect the content, and all legal disclaimers that apply to the journal pertain.

© 2020 Published by Elsevier Ltd.

CRediT author statement

Nesrine Saidani: Investigation; Writing - Review & Editing **Emilia Morallón:** Resources, Writing - Review & Editing, Funding acquisition; **Francisco Huerta:** Formal analysis, Data Curation, Writing - Review & Editing, Supervision, **Salma Besbes-Hentati:** Writing - Review & Editing, Supervision, Funding acquisition; **Francisco Montilla:** Conceptualization, Methodology, Validation, Formal analysis, Resources, Data Curation, Writing - Original Draft, Supervision

Electrochemical Synthesis of Fluorinated Polyanilines

*Nesrine Saidani^{1,2}, Emilia Morallón², Francisco Huerta³, Salma Besbes-Hentati¹, Francisco
Montilla^{2,*}*

¹University of Carthage, Faculty of Sciences of Bizerte, LR13ES08, Laboratory of Materials Chemistry, Tunisia

²Departamento de Química Física e Instituto Universitario de Materiales de Alicante. Universidad de Alicante. Apdo. de Correos 99, E-03080 Alicante, Spain

³Departamento de Ingeniería Textil y Papelera, Universitat Politècnica de Valencia, Plaza Ferrandiz y Carbonell, 1, E-03801 Alcoy, Spain.

Keywords: Conducting polymers; electrochemical copolymerization; fluoroaniline; monomer reactivity

* francisco.montilla@ua.es

ABSTRACT

A set of fluoro-functionalized polyaniline conducting polymers was synthesized by cyclic scanning of the potential from acidic solutions containing aniline and 2-fluoroaniline monomers. The monomer feed ratio was varied to modulate the composition of the synthesized materials. The fluorination level of the copolymers was quantified from X-ray photoelectron spectroscopy. The upper inversion potential of the cyclic scans was proved as a suitable tool to tune the fluorination level, as the reactivity of the growing chains depends strongly on that experimental parameter. We found that terminal fluorinated anilines present a reactivity for homocoupling 5 times lower than for heterocoupling, independently of the limiting potential. Conversely, aniline terminal groups present a reactivity strongly dependent on the limiting potential, favoring the heterocoupling reactions at high inversion potentials. The maximum fluorination level of polyaniline rings achieved is about 75%.

1. Introduction

Electroactive conducting polymers (ECP) are materials that can be designed with high molecular precision to be implemented in a huge variety of applications such as electrochromic systems, chemical sensors, rechargeable batteries, electromagnetic shielding or optoelectronic devices, among others [1]. ECP are usually synthesized from their parent monomers by either chemical or electrochemical oxidative polymerization. It is well known that some physicochemical properties of ECP such as electron conductivity, bandgap or thermal stability can be tuned by incorporating functional groups to the polymer backbone. Such a modification can be achieved by polymerization of previously functionalized monomers or in an additional step after polymerization [2–4]. The result can be the enhancement of specific polymer properties, thus opening its applications to fields like charge storage, electrochemical sensing or corrosion protection among others [5–9].

Plastic polymers and rubbers functionalized with fluorine have attracted scientific and technological interest for years owing to their high thermal stability and hydrophobicity. On the contrary, minor attention has been paid to the synthesis and characterization of fluorinated ECP. The very low polarizability, high electronegativity and low van der Waals radius of fluorine together with its strong electron-withdrawing character, makes this heteroatom attractive to modulate the optoelectronic properties of conjugated polymers [10–13]. Besides, fluorine is an effective resonance donating species that can lead to low-gap ECP, whereas its electrostatic interactions with other species (such as $F\cdots H$, $F\cdots S$, and $F\cdots \pi$) can be used to modify physical properties of thin-film-based devices [14–16].

Among ECP, polyaniline (PANI) and its copolymers are probably the most investigated materials due to their low cost, high environmental stability, high electrical conductivity and

wide range of applications [17–21]. As occurs to other fluorinated ECP, fluorinated polyanilines have not been characterized in-depth despite they were proposed as chemical stable substrates for the immobilization of proteins, humidity sensors, oxygen selective membranes or superhydrophobic surfaces [22–28].

The objectives of this work are to electrosynthesize fluorinated polyanilines and to provide an electrochemical method to determine the fluorination level of the polymers. Fluorinated polyanilines will be deposited by potentiodynamic oxidation in acidic aqueous solution and the effect of some synthesis parameters, such as the inversion potential and the composition of the precursor solution, on the properties of the deposited material will be discussed in the light of voltammetric and spectroscopic results.

2. Experimental part

2-fluoroaniline (2FA) and Aniline (ANI) (Sigma-Aldrich) were distilled before used, sulfuric acid (98% purity, for analysis) was purchased from Merck. All solutions were prepared with ultrapure water obtained from an ELGA Lab Water Purelab system (18.2 M Ω cm). The electrochemical experiments were performed in conventional electrochemical glass cells which were purged by bubbling a N₂ flow and this atmosphere was maintained during all the experiments. The working electrodes were indium-tin oxide (ITO) on glass substrates (Delta, sheet resistance = 15–25 Ω/\square) electrodes that were degreased by sonication in an acetone bath for 10 min and rinsed with abundant ultrapure water. The counter electrode was a platinum wire. All potentials were measured against a reversible hydrogen electrode (RHE) immersed in the working solution through a Luggin capillary. Electrochemical experiments were performed with an eDAQ Potentiostat (EA163 model) coupled to EG&G Parc Model

175 wave generator and the data acquisition was performed with eDAQ e-corder 410 unit (Chart and Scope Software). UV-vis spectroscopy was performed with an Ocean Optics spectrophotometer (Flame model) using an Avantes DH-2000 Deuterium–Halogen light source. X-ray photoelectron spectroscopy (XPS) was measured with a VG-Microtech Multilab 3000 electron spectrometer using a non-monochromatized Mg-K α (1253.6 eV) radiation source of 300 W and a hemispheric electron analyzer equipped with nine channel electron multipliers. The pressure of the analysis chamber during the scans was about 5×10^{-7} Pa. After the survey spectra were obtained, higher resolution survey scans were performed at pass energy of 50 eV. The intensities of the different contributions were obtained by calculation of the integral of each peak, after having eliminated the baseline with S form and adjusting the experimental curves to a combination of Lorentz (30%) and Gaussian (70%) lines. Bond energies were referred to the C 1s line at 284.4 eV and the values were obtained with ± 0.2 eV precision. Morphology of the modified electrodes was determined by field emission scanning electron microscopy (FESEM, ZEISS model Merlin VP Compact).

3. Results and discussion

3.1. Electrochemical homopolymerization of 2-fluoroaniline

Fig. 1 shows cyclic voltammetry curves recorded for an ITO electrode within a 0.05-1.15 V potential window in 0.5 M H₂SO₄ medium containing 0.1 M 2-fluoroaniline. The rise of an anodic current at about 1.0 V during the first forward scan can be ascribed to the oxidation of monomer. In the reverse sweep, two cathodic peaks appear at 0.50 V and 0.73 V coming from the reduction of those species formed after the oxidation of 2FA. Both cathodic features show anodic counterparts at 0.55 V and 0.76 V as observed in the subsequent

positive-going scans. Besides, the global voltammetric charge associated with these peaks increases upon cycling, thus suggesting the formation of an electroactive polymer film on the ITO surface.

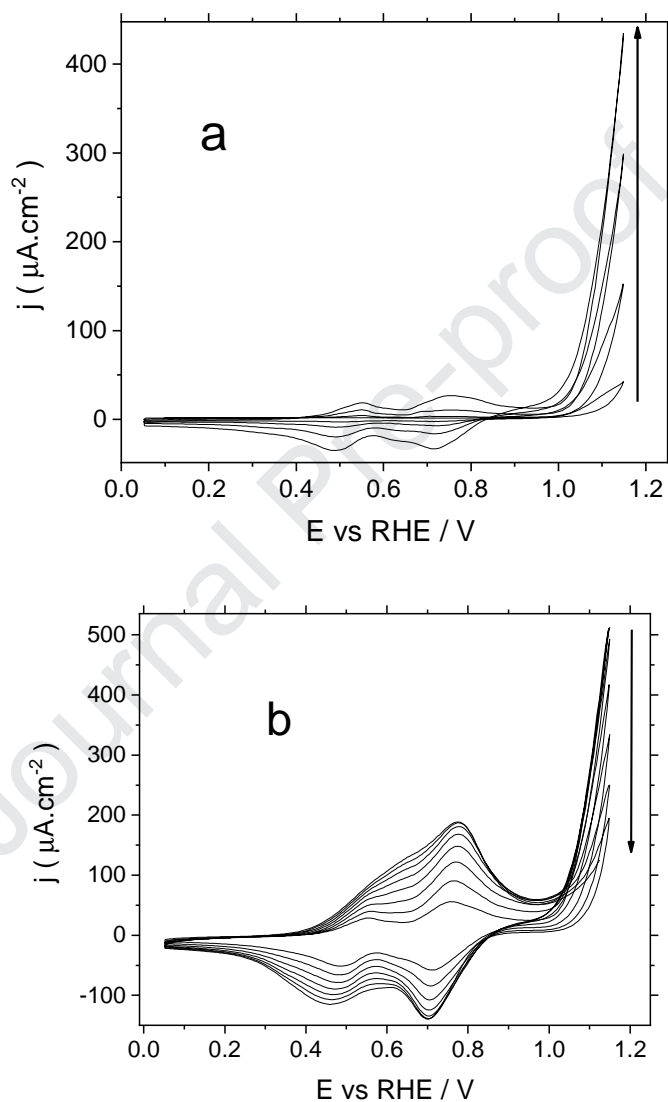


Figure 1. Cyclic voltammograms recorded for an ITO electrode immersed in 0.5 M H_2SO_4 medium containing 0.1 M 2-fluoroaniline. Scan rate 100 mVs^{-1} . (a) cycles 1st to 4th (b) cycles 5th to 11th.

In a way similar to PANI, the growth of poly-2-fluoroaniline during the first potential cycles looks autocatalytic, as deduced from both the continuous increase of the monomer oxidation current and the lower potential needed to trigger oxidation on successive scans. Unexpectedly such a tendency breaks, as the monomer oxidation current decreases progressively from the fifth potential scan (see Fig. 1b). Besides, in the scan to more positive potentials, a wide peak appears at 0.78 V and, finally, a stable response is obtained after 11 potential cycles. This response differs strongly from that of a conventional PANI growth and points that poly-2-fluoroaniline could be formed by oligomeric chains, probably shorter than those expected for a true polymeric product. The possibility that low electrical conductivity of the deposited material could hinder further oxidation of monomers cannot be ruled out [27].

Once the deposition of the material was complete, the electrode was removed from the electrochemical cell, rinsed with ultrapure water and transferred to a background 0.1 M H_2SO_4 solution free of monomer. Fig. 2 shows the stabilized voltammogram obtained under those conditions, where just a broad single anodic peak centered at 0.78 V can be discerned and, besides, two overlapped features peaking at 0.48 V and 0.62 V appear in the cathodic section of the cyclic voltammetry.

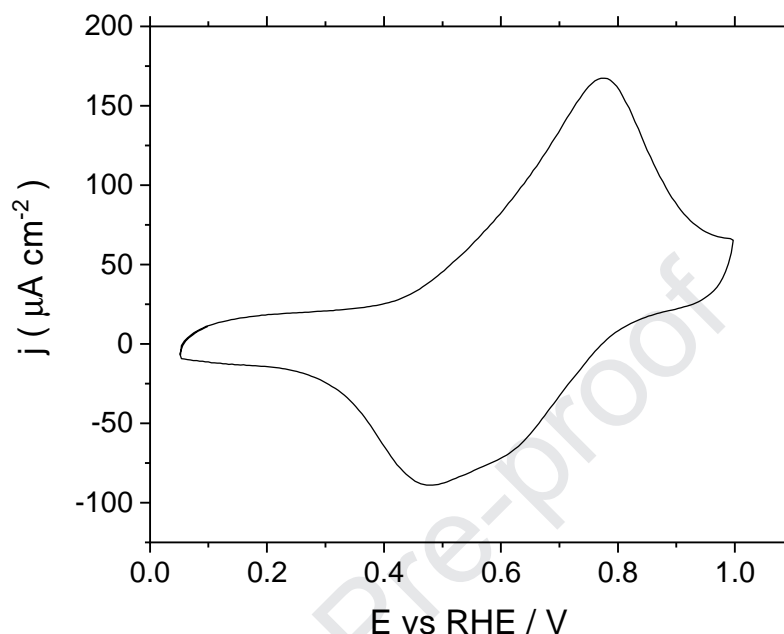


Figure 2. Stabilized cyclic voltammogram of an ITO electrode covered with a layer of poly-2FA in 0.1 M H₂SO₄ background solution. Scan rate 100 mV s⁻¹.

The shape of this voltammogram reminds the well-known electrochemical behavior of PANI in sulfuric acid medium [29], although the anodic peak is, in this case, shifted more than 200 mV to higher potential values. This shifting could be explained by the fluorine inductive effect that decreases the electronic density of the aromatic rings. This effect is commonly observed in other fluorinated conjugated polymers, where the fluorine atom drives to an increase in the HOMO energy level of the conjugated chains [30,31]. Consequently, the oxidation onset for the fluorinated polymers occurs at higher potentials than those of the

parent materials [32,33]. This is the case of fluorinated PANI, whose oxidation potential appears at around 0.3 V above the PANI doping.

3.2. *Electrochemical copolymerization of 2FA and aniline*

It is known that the composition of chemically synthesized aniline copolymers depends strongly on the reactivity of each comonomer [34], a feature that is difficult to modulate. However, some control over copolymerization can be exerted in electro-copolymerization by experimental parameters such as the applied potential [35] or the monomer feed composition [36]. Hence, using aniline as the comonomer for its copolymerization with 2-fluoroaniline, the feed ratio of the latter species, f_{2FA} , can be defined as the molar content in 2FA relative to the total molar amount of monomers present in the working solution:

$$f_{2FA} = \frac{[2FA]}{[2FA] + [ANI]} \quad \text{Eq. (1)}$$

Different feed ratios were employed in this work: 0.5, 0.66, 0.83 and 0.91, which are equivalent to 2FA:ANI molar ratios of 1:1, 2:1, 5:1 and 10:1, respectively. The total concentration of monomer species, $[2FA] + [ANI]$, was 0.1 M in all cases. Fig. 3 shows cyclic voltammograms recorded during the electrochemical copolymerization of aniline and 2FA at $f_{2FA} = 0.5$. The polymer growth occurs after triggering the oxidation of monomers at a potential beyond 1.0V. In this case, the shape of the voltammetric curves is very similar to that recorded during the electrochemical growth of PANI (see Fig. S1 in the supporting information). The characteristic leucomeraldine-emeraldine redox transformation dominates the voltammetric profile appearing as an intense pair of peaks centered at around 0.4 V. The

polymer was grown during 40 scans until this anodic feature reached a peak current close to 0.2 mA cm^{-2} . This result reveals that the copolymerization process is slower than the homopolymerization of aniline monomer since similar current values were obtained after only 12 potential scans.

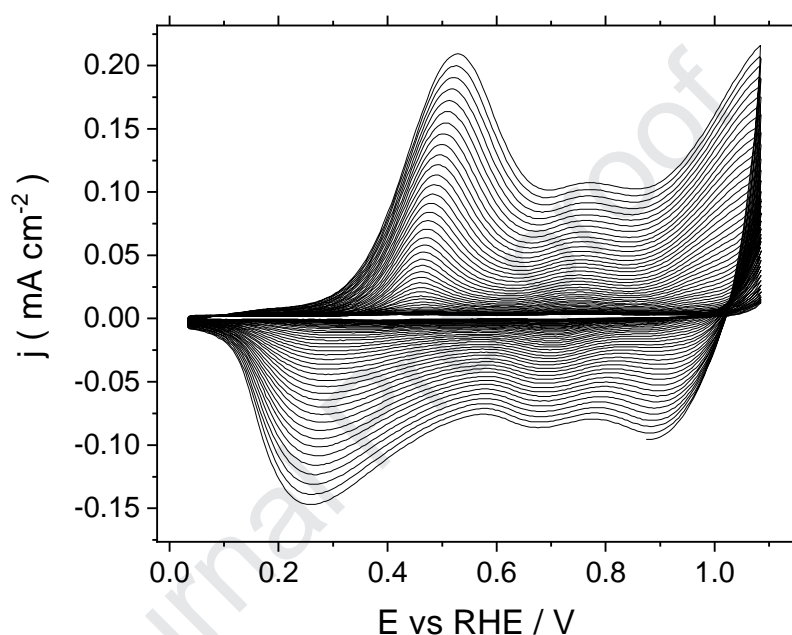


Figure 3. Cyclic voltammograms recorded for an ITO electrode during the electro-copolymerization of a mixture 0.05 M 2-fluoroaniline + 0.05 M aniline ($f_{2FA}= 0.5$) in 0.5 M H_2SO_4 . Scan rate 100 mVs^{-1} . Inversion potential 1.1 V.

To determine the chemical composition of the copolymer, a film-modified electrode was rinsed with ultrapure water, dried under nitrogen, stored in a dry place for 24 h and then analyzed by XPS. Fig. 4 shows the high-resolution spectra obtained for C1s, N1s and F1s signals. The best fit for the C1s signal includes a major band at 284.6 eV, two minor bands at

285.6 and 287.0 eV and, finally, a very weak feature at 290.9 eV. The main contribution corresponds unambiguously to aromatic carbon, whereas the two minor peaks are assigned to carbon bound to either neutral or positively-charged nitrogen, respectively [37]. The high binding energy of the weak intensity peak, despite being within the detection limit of the technique, could indicate the presence of carbon bound to F atoms [38]. On the other hand, the N1s spectrum can be deconvoluted into one major peak at 398.4 eV and two minor features at 399.5 and 400.5 eV. The contribution at 398.4 eV corresponds to unprotonated quinone imine species [39] which, in agreement with the assignment suggested above for the C1s feature at 285.6 eV, seems the main form of N in the polymer. The peak at 399.5 eV corresponds to the presence of neutral secondary amine [39] and the higher signal, at 400.5 eV can be attributed to protonated nitrogen species which are in a lower relative amount [40].

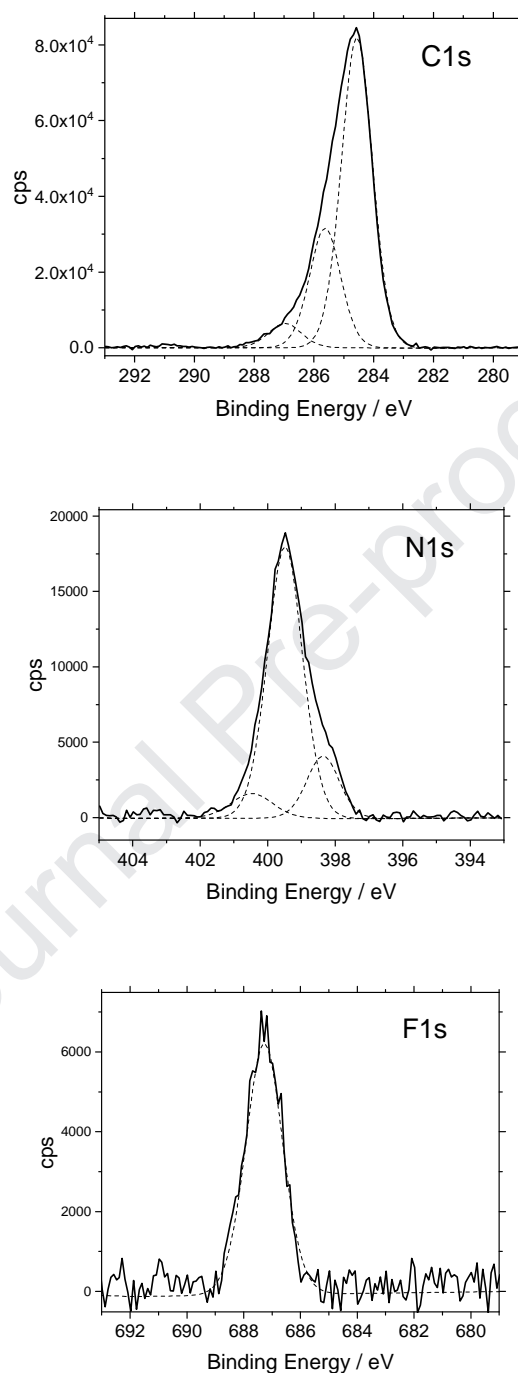
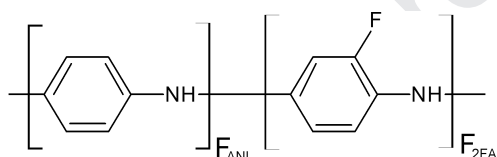


Figure 4. High-resolution X-ray photoelectron spectra obtained from C1s, N1s and F1s signals for a poly(ANI-co-2FA) copolymer synthesized as in Fig. 3.

Concerning the F1s signal, the XPS reveals a single chemical environment that corresponds to a C-F bond [41]. The relative intensities of photoelectronic transitions for fluorine and nitrogen can be used to assess the atomic composition of the material and, from that value, to quantify the incorporation of 2FA monomers to the copolymer. A general structure for the neutral state of the polymeric chain of poly(ANI-co-2FA) is visualized in Scheme 1, where F_{2FA} represents the molar fraction of 2-fluoroaniline (fluorination level) within the polymer.



Scheme 1

The effect of the upper inversion potential on the composition of the material and hence on the fluorination level can be observed in table 1 for a feed ratio $f_{2FA}=0.5$. The chart reveals that fluorination increases from 16% up to 24% as the upper inversion potential is extended, correspondingly, from 1.10 V up to 1.20 V. This result suggests a simple way to tune the copolymer composition with no need to change the feed composition.

Table 1. Effect of the inversion potential (E_{limit}) on the atomic composition of poly(ANI-co-2FA) copolymers and their fluorination level (F_{2FA}) from XPS quantitative analysis. Other experimental conditions of synthesis as in Fig. 3.

f_{2FA}	$E_{\text{limit}} / \text{V}$	Elemental composition / at%			F_{2FA}	Atomic Formula
		C	N	F		
0.5	1.10	84.0	9.8	1.6	0.16	$\text{C}_{17.2}\text{N}_2\text{H}_x\text{F}_{0.32}$
	1.15	83.1	10.8	2.0	0.18	$\text{C}_{15.4}\text{N}_2\text{H}_x\text{F}_{0.36}$
	1.20	81.1	10.1	2.4	0.24	$\text{C}_{16.1}\text{N}_2\text{H}_x\text{F}_{0.48}$
0.66	1.10	77.4	10.6	2.8	0.26	$\text{C}_{14.6}\text{N}_2\text{H}_x\text{F}_{0.52}$
	1.15	80.2	11.0	3.4	0.31	$\text{C}_{14.6}\text{N}_2\text{H}_x\text{F}_{0.62}$
	1.20	79.6	10.5	4.6	0.44	$\text{C}_{15.2}\text{N}_2\text{H}_x\text{F}_{0.87}$
0.83	1.10	79.1	10.0	5.6	0.57	$\text{C}_{15.8}\text{N}_2\text{H}_x\text{F}_{1.1}$
	1.15	79.3	10.4	5.4	0.52	$\text{C}_{15.2}\text{N}_2\text{H}_x\text{F}_{1.0}$
	1.20	79.1	11.0	6.0	0.55	$\text{C}_{14.4}\text{N}_2\text{H}_x\text{F}_{1.1}$
0.91	1.10	75.5	9.9	6.7	0.68	$\text{C}_{15.2}\text{N}_2\text{H}_x\text{F}_{1.4}$
	1.15	77.5	10.1	7.1	0.71	$\text{C}_{15.3}\text{N}_2\text{H}_x\text{F}_{1.4}$
	1.20	72.3	8.5	6.5	0.76	$\text{C}_{16.9}\text{N}_2\text{H}_x\text{F}_{1.5}$

The electrochemical responses of fluorinated materials are compared in Fig. 5. The stabilized voltammograms look quite similar to those of unmodified PANI in the same electrolyte. The first anodic peak appearing at around 0.5 V for the three copolymer samples is assigned to a leucoemeraldine-emeraldine transition. The rise of a second redox peak takes place at 0.78 V, when the copolymer is synthesized at higher upper inversion potentials. Figs. 1 and 2 reveal that this peak is characteristic of poly-2FA homopolymer, a fact that suggests

the presence of fluorinated rings in the copolymer although some contribution to this voltammetric peak may arise from quinone and/or phenazine structures in PANI [42,43].

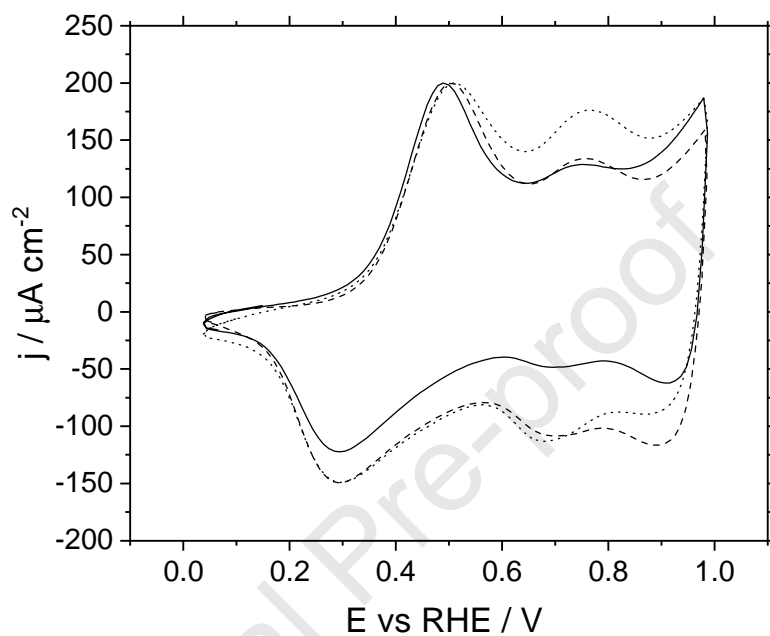


Figure 5. Cyclic voltammograms recorded in a background 0.1 M H_2SO_4 solution showing the response of poly(ANI-co-2FA) polymers deposited at 1.1V (solid line), 1.15 V (dashed line) and 1.20 V (dotted line) upper inversion potentials for a feed ratio $f_{2\text{FA}}=0.5$. Scan rate 100 mV s^{-1} .

A set of poly(ANI-co-2FA) copolymers was deposited potentiodynamically on ITO with a combination of increasing anodic limits (1.10, 1.15 and 1.20 V) and higher monomer feed ratios ($f_{2\text{FA}}=0.66$, 0.83 and 0.91). The corresponding cyclic voltammograms recorded during potentiodynamic polymerizations are shown in Fig. S2. The atomic composition of the resulting materials was determined by XPS and the results are collected in table 1. As for homopolymers formed from 2FA, the C1s signal of all copolymer samples show a small

contribution, close to 292 eV, that can be ascribed to the presence of C-F bonds, thus proving the success of the copolymerization reaction under different experimental conditions. As expected, table 1 shows that an increase in either 2FA feed ratio or upper inversion potential results in a higher fluorine content within the deposited film. Data from table 1 are plotted in Fig. 6 to visualize better the actual relation between the composition of the polymerization solution expressed as f_{2FA} , and that of the copolymer product expressed in terms of F_{2FA} .

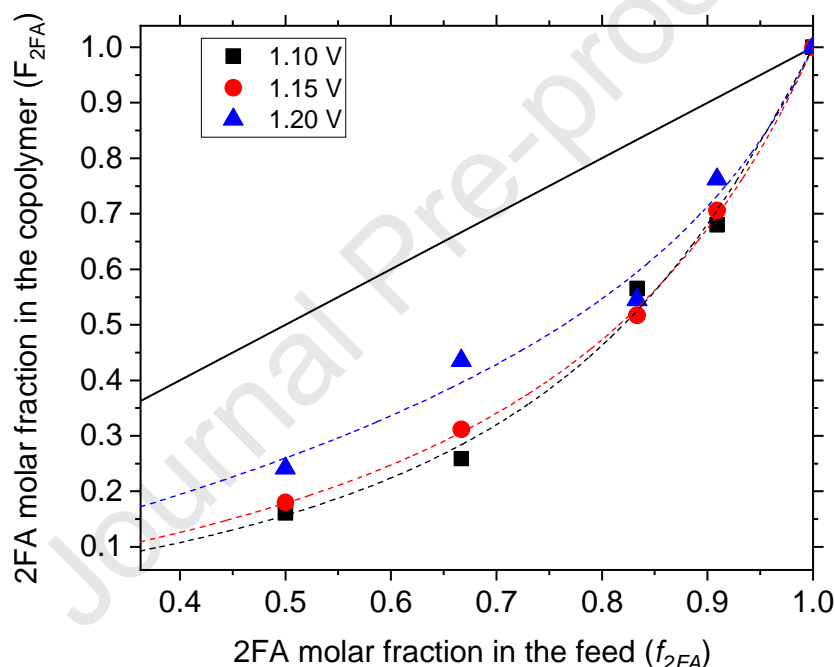
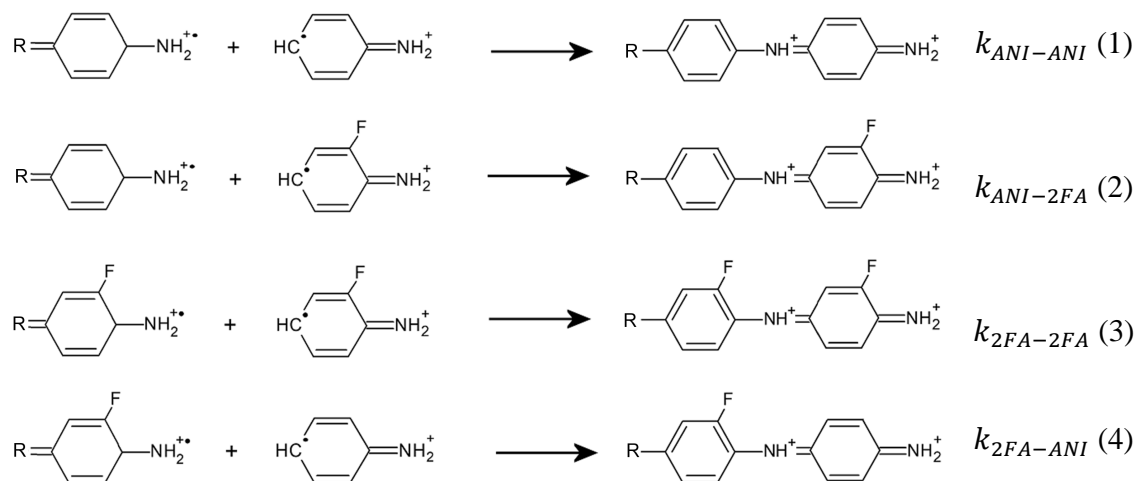


Figure 6. Fluorination level of poly(ANI-co-2FA) copolymer as a function of the chemical composition of the feed solution for different upper inversion potentials (indicated in the figure). Dotted lines show the fitting of Dostal model (as cited by Cowie [44]) to experimental values. A solid line represents a hypothetical same reactivity for 2FA and ANI.

The solid line in Fig. 6 represents the unit slope and corresponds to the hypothetical case that 2FA and ANI comonomers show the same reactivity, i.e. they both incorporate to the copolymer in the same proportion they are present in the feed solution. Since the actual values of F_{2FA} appear always below the solid line, it can be derived that 2FA is less reactive than ANI.

Further analysis of monomer reactivity can be performed by fitting the values of F_{2FA} in Fig. 6 to the terminal copolymerization model proposed by Dostal (cited by Cowie [44]). It can be assumed that the polymer growth rate depends on both the terminal ring at the growing chain and the monomer to be incorporated (either ANI or 2FA). Accordingly, four different coupling reactions can lead to the propagation of the copolymer chain, each one characterized by its kinetic constant [34,45] as depicted in Scheme 2.



Scheme 2: Possible coupling reactions of ANI and 2FA

Based on this growth model, a kinetic expression can be proposed (Eq. 2) that relates the copolymer composition in terms of F_{2FA} with the mole fraction of each comonomer in the feed and with the kinetic constants of the four possible couplings:

$$F_{2FA} = \frac{r_{2FA} \cdot f_{2FA}^2 + f_{2FA} \cdot f_{ANI}}{r_{2FA} \cdot f_{2FA}^2 + 2f_{2FA} \cdot f_{ANI} + r_{ANI} \cdot f_{ANI}^2} \quad (\text{Eq. 2})$$

being $r_{ANI} = \left(\frac{k_{ANI-ANI}}{k_{ANI-2FA}} \right)$ the reactivity ratio for ANI-terminated chains (reactions 1 and 2) and, correspondingly, $r_{2FA} = \left(\frac{k_{2FA-2FA}}{k_{2FA-ANI}} \right)$ the reactivity ratio for 2FA-terminated chains (reactions 3 and 4). The experimental data in Fig. 6 were fitted to Eq. 2 and the resulting reactivity ratios are presented in table 2 as a function of the inversion potential. For copolymer chains containing 2FA reactive endings, the values of r_{2FA} are close to 0.25, thus revealing that the rate of homocoupling through 2FA addition (reaction 3) is about 4 times lower than that of heterocoupling (reaction 4), irrespective of the inversion potential employed. This result supports the voltammetric suggestion that the fluoro-functionalized monomer is less reactive than aniline to the same extent at any potential.

Table 2. Effect of the inversion potential (E_{limit}) on the reactivity ratio of poly(ANI-co-2FA) chains terminated in either 2FA (r_{2FA}) or ANI (r_{ANI}).

$E_{\text{limit}} / \text{V}$	r_{2FA}	r_{ANI}
1.10	0.283	5.89
1.15	0.237	4.68
1.20	0.243	2.54

The picture is quite different for polymer chains containing aniline endings because, on the one hand, homocoupling is preferred against heterocoupling (r_{ANI} is always higher than 1) and, on the other hand, the incorporation of 2FA seems favored at increasing inversion potentials (r_{ANI} falls at higher E_{limit}).

In conclusion, the copolymer growth takes place mainly through ANI-terminated chains which show reactivities strongly influenced by the upper potential limit employed. Since the incorporation of aniline monomers to these chains (homopolymerization) is faster at lower inversion potentials, to attain higher fluorination level of the end product, higher potentials should be employed. Fig. 7 shows an analysis of the voltammetric response for a set of copolymers in the background electrolyte revealing the combined effect of the more significant electrosynthesis parameters, $f_{2\text{FA}}$ and E_{limit} . At the lower feed ratio of 2FA monomer, the shape of cyclic voltammogram is strongly dependent on the upper inversion potential reached. The intensity of the peak at around 0.8 V rises, thus showing a higher fluorination level at increasing E_{limit} . The use of increasing feed ratios of 2FA monomer makes the voltammetric profiles dominated by the peak around 0.8 V which overlaps the features related to leucoemeraldine-emeraldine transitions.

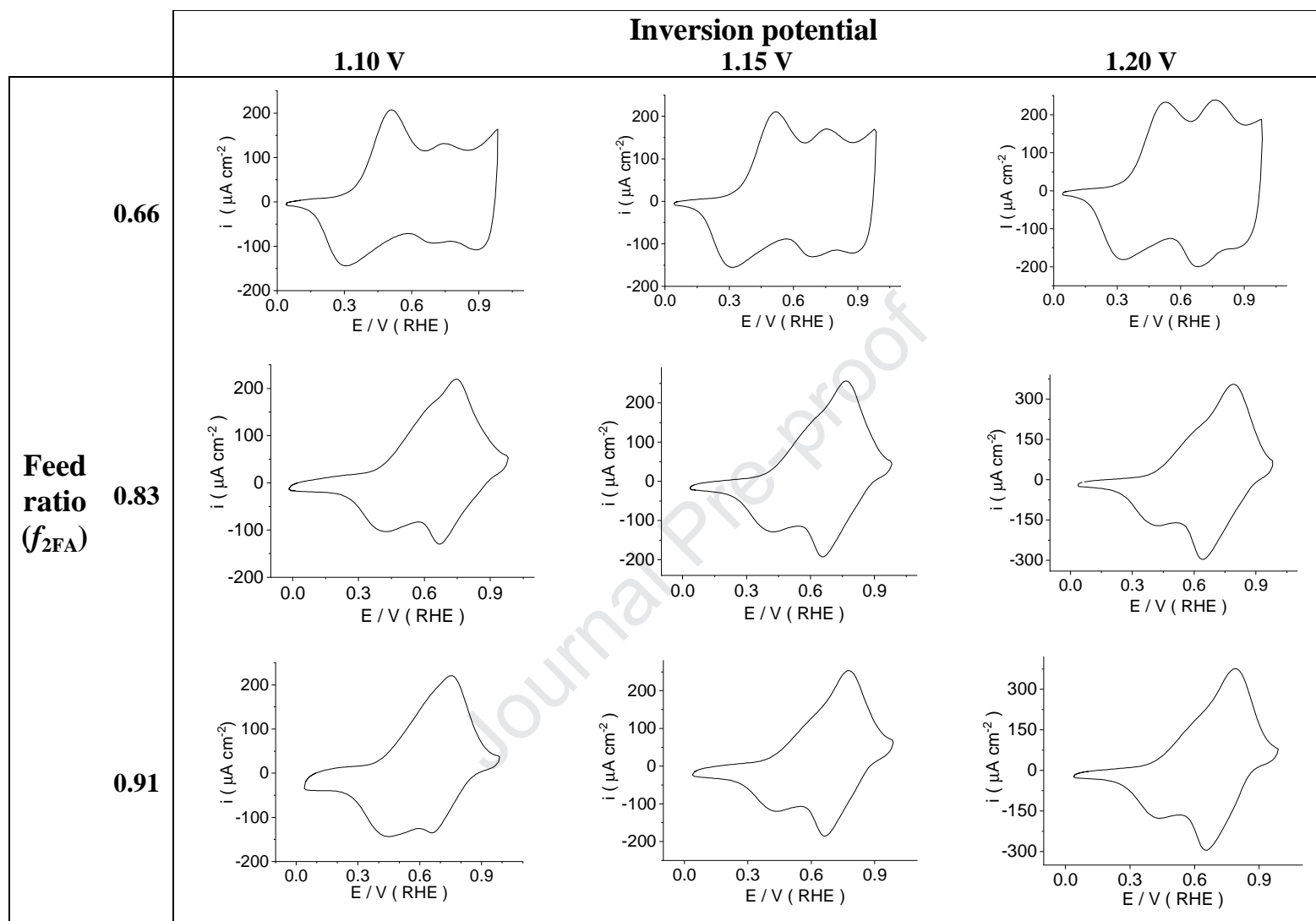


Figure 7. Stabilized cyclic voltammograms for poly(ANI-co-2FA) copolymers synthesized at different upper inversion potentials and 2FA monomer feed ratios in 0.1 M H₂SO₄ background solutions. Scan rate 100 mV s⁻¹.

Both overlapped contributions, the peak around 0.8 V (F peak) and the leucoemeraldine-emeraldine peak (LE peak) can be deconvoluted using a Gaussian function. Fig. 8a shows the cyclic voltammogram recorded at $f_{2FA} = 0.83$ and $E_{limit} = 1.15$ V with the deconvoluted peaks showing the voltammetric charge under the LE peak, Q_{LE} , and the voltammetric charge under the high potential peak Q_F (ascribed to the presence of F-substituted rings).

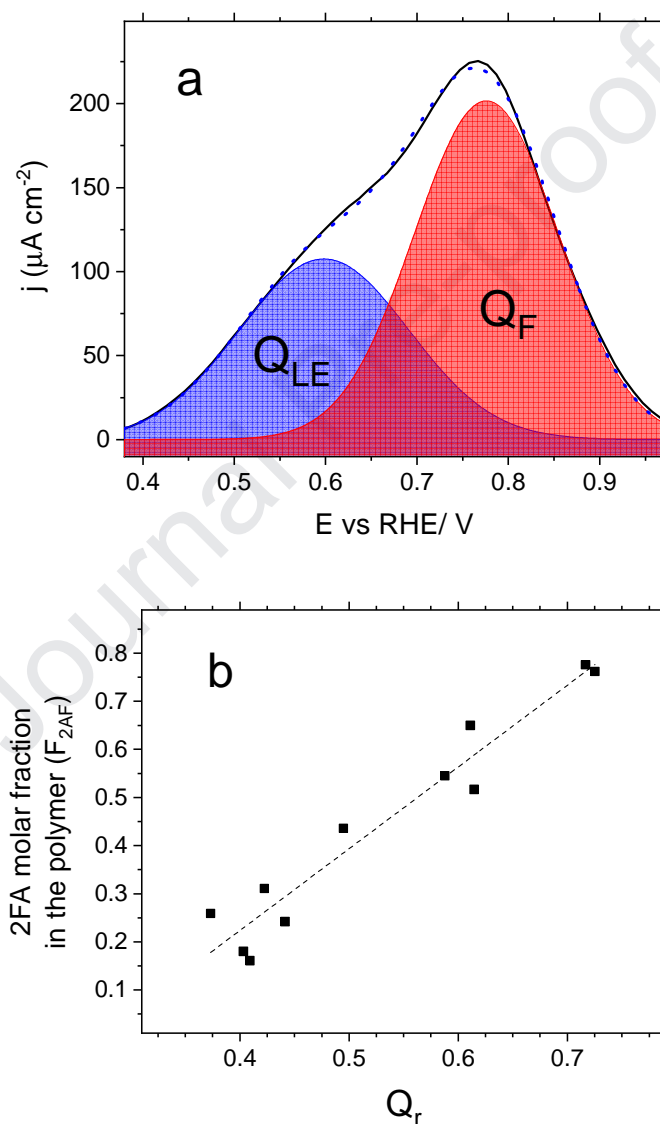


Figure 8. (a) Gaussian deconvolution of the forward scan for a poly(ANI-co-2FA) synthesized at $f_{2FA} = 0.83$ and $E_{limit} = 1.15$ V; (b) Copolymer fluorination level against Q_r , the voltammetric charge under the fluorine peak (Q_F) relative to the total charge ($Q_F + Q_{LE}$) obtained for all the copolymers synthesized in this work.

We can define Q_r as the ratio between Q_F , and the total charge recorded in the forward scan ($Q_F + Q_{LE}$). Fig 8b plots Q_r against the molar ratio of fluorine-functionalized units in the copolymer as determined by XPS, F_{2FA} . The plot follows a linear trend, $F_{2AF} = 1.70 \times Q_r - 0.45$, which means that the fluorination level of a poly(ANI-co-2FA) copolymer can be easily determined from voltammetric experiments.

The surface morphology of PANI and poly(ANI-co-2FA) films deposited up to 1.15 V onto ITO electrodes is compared in Fig. 9 at the same magnification.

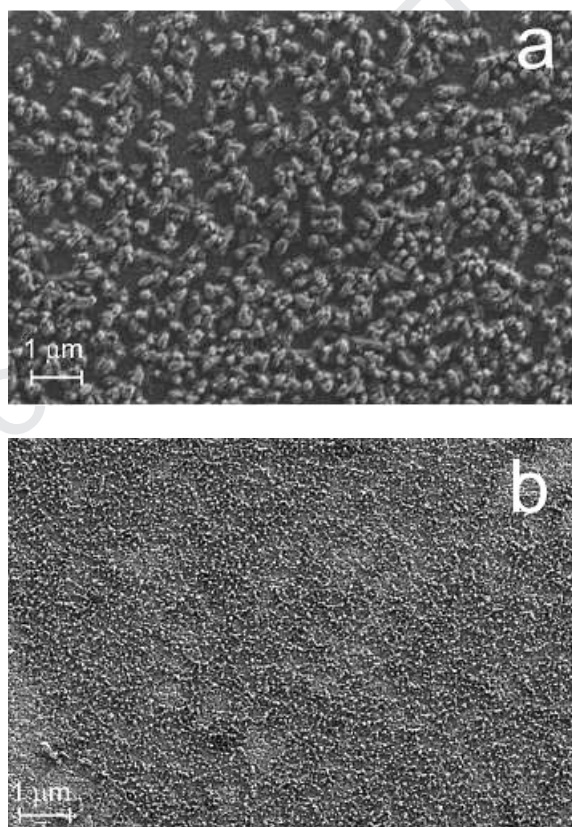


Figure 9. SEM images of PANI (A) and poly(ANI-co-2FA) (B) modified electrode synthesized at $f_{2FA} = 0.83$ and $E_{limit} = 1.15$ V. Magnification: 10000x

Both polymeric materials consist of three-dimensional arrangements of loosely packed, almost globular structures, which appear uniformly distributed over the surface of the ITO substrate. The main difference arises in the size of the globules which, for PANI are about 150-250 nm in width whereas the poly(ANI-co-2FA) copolymer shows smaller features by a factor close to 5. These differences can be ascribed to the rate of electrochemical deposition, which is significantly higher for PANI under the same experimental conditions (upper inversion potential, scan rate and the total concentration of monomer).

The electronic absorption spectra of these two polymers are presented in Fig. 10. They are characterized by features such as the π - π^* transition of benzenoid rings which occurs roughly 320 nm below the ITO spectral cutoff [46]. Besides, the doped states of PANI (black solid line) show two characteristic absorption bands above 400 nm [47]. The first one is a clear-cut absorption centered at 450 nm that was formerly ascribed to the transition from the lower-lying band to the polaron band in semi-oxidized PANI chains [48]. The other one is a broad feature at around 770 nm, which is often described as an electronic transition from the valence band to the polaron band [48,49]. Interestingly, the 450 nm band is shifted 18 nm to lower energy for the copolymer (red dashed line). Redshifts are commonly understood in terms of an increase in the conjugation length of the absorbing polymeric species. According to this interpretation, it is believed that the presence of fluorine atoms could favor the planarity of poly(ANI-co-2FA) chains giving rise to an extended conjugation. Additional minor bands are observed at 715 and 770 nm. The wavelength of the latter one matches with the position of the polaron in PANI, which suggests the presence of some non-fluorinated domains or blocks within the copolymer films. The band at 715 nm can be assigned to the n - π^* transition of quinoid rings [50]. It should be also noted that the lack of electronic absorptions coming from the copolymer material at the low energy end of the UV-visible spectrum suggests these transitions are shifted down to the NIR region.

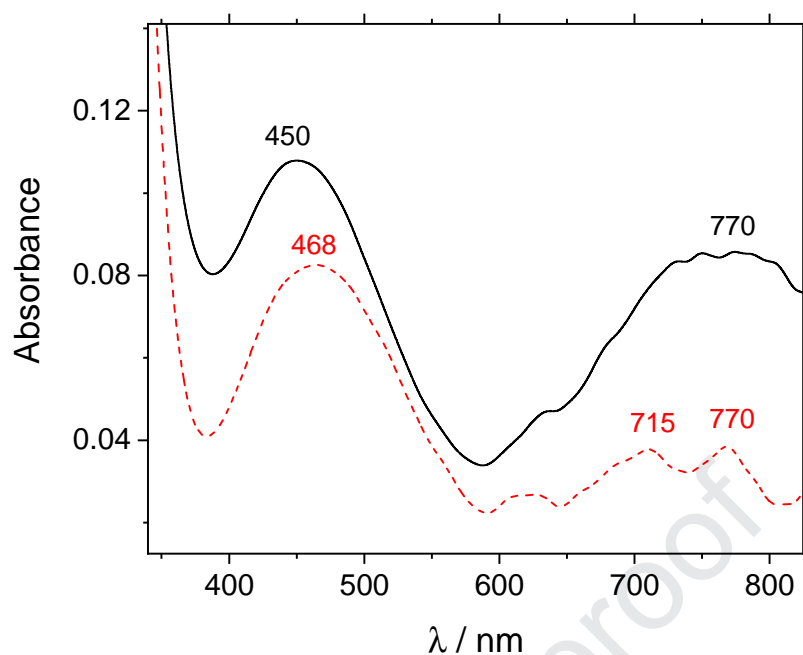


Figure 10. UV-vis spectra of PANI (black solid) and poly(ANI-co-2FA) (red dashed) synthesized at $f_{2\text{FA}} = 0.83$ and $E_{\text{limit}} = 1.15$ V on ITO. Both spectra were obtained at 0.85 V.

4. Conclusion

The electrochemical synthesis of fluorinated polyaniline can be carried out from acidic solutions containing either 2-fluoroaniline monomers (homopolymerization) or mixtures of aniline and fluorinated monomers (copolymerization). The homopolymerization process yields probably a short-chain polymer (oligomer) fluorinated in all rings as the end product. This material shows a particular voltammetric response, as only one redox peak appears at intermediate potentials between those attributed in PANI to leucoemeraldine-emeraldine and emeraldine-pernigraniline transitions.

Fluorinated polyaniline or poly(ANI-co-2FA) copolymer, shows voltammetric peaks resembling those of PANI and, besides, singular middle peaks coming from fluorinated chains. The reactivity of the 2-fluoroaniline monomer is much lower than that of aniline but

the fluorination level of the copolymer can be controlled by changing the monomer feed ratio in the polymerization solution. Besides, the upper inversion potential of the potentiodynamic scan constitutes a supplementary electrochemical tool to tune the fluorine content because the reactivity ratio of ANI-terminated chains within the copolymer is strongly dependent on this electrochemical parameter, whereas those terminated on fluorinated rings show an almost constant reactivity ratio.

The surface morphology of both materials seems rather similar but it reveals the higher rate of polyaniline deposition. The electrochemical copolymerization method yields maximum fluorine content in the end product of about 0.76 F atoms per N atom (3 in 4 rings come from 2FA monomers). A suitable analysis of cyclic voltammetry results, including peak deconvolution, can be used to estimate easily the fluorination level of copolymer samples. The presence of fluorine seems to increase the conjugation length of copolymer chains by promoting their planarity, but the surface morphology is slightly affected.

Acknowledgments

The authors wish to thank Generalitat Valenciana (PROMETEO/2018/087) for financial support. Nesrine Saidani would like to thank the Tunisian Ministry of Higher Education and Research for funding her stay at the University of Alicante.

References

- [1] T.A. Skotheim, J.R. Reynolds, eds., *Handbook of Conducting Polymers: Conjugated Polymers: Processing and Applications*, 4th ed., CRC Press, 2006.
- [2] M. Jaymand, *Prog. Polym. Sci.* 38 (2013) 1287–1306.
- [3] C. Barbero, H.J. Salavagione, D.F. Acevedo, D.E. Grumelli, F. Garay, G.A. Planes, G.M. Morales, M.C. Miras, *Electrochim. Acta* 49 (2004) 3671–3686.
- [4] J. Quílez-Bermejo, A. Ghisolfi, D. Grau-Marín, E. San-Fabián, E. Morallón, D. Cazorla-Amorós, *Eur. Polym. J.* 119 (2019) 272–280.
- [5] C. Chen, Z. Gan, C. Xu, L. Lu, Y. Liu, Y. Gao, *Electrochim. Acta* 252 (2017) 226–234.
- [6] C. Chen, G. Ding, D. Zhou, X. Lu, *Electrochim. Acta* 97 (2013) 112–119.
- [7] L. Qiu, S. Zhang, L. Zhang, M. Sun, W. Wang, *Electrochim. Acta* 55 (2010) 4632–4636.
- [8] R. Zhao, L. Zhu, Y. Cao, X. Ai, H.X. Yang, *Electrochem. Commun.* 21 (2012) 36–38.
- [9] B. Narayanasamy, S. Rajendran, *Prog. Org. Coatings* 67 (2010) 246–254.
- [10] W. Lu, J. Kuwabara, T. Iijima, H. Hirgashimura, H. Hayashi, T. Kanbara, *Macromolecules* 45 (2012) 4128–4133.
- [11] X. Li, X. Liu, P. Sun, Y. Feng, H. Shan, X. Wu, J. Xu, C. Huang, Z.K. Chen, Z.X. Xu, *RSC Adv.* 7 (2017) 17076–17084.
- [12] Q. Zhang, M.A. Kelly, N. Bauer, W. You, *Acc. Chem. Res.* 50 (2017) 2401–2409.
- [13] H. Zhou, L. Yang, A.C. Stuart, S.C. Price, S. Liu, W. You, *Angew. Chemie - Int. Ed.* 50 (2011) 2995–2998.

- [14] B. Nketia-Yawson, H.S. Lee, D. Seo, Y. Yoon, W.T. Park, K. Kwak, H.J. Son, B. Kim, Y.Y. Noh, *Adv. Mater.* 27 (2015) 3045–3052.
- [15] K. Do, Q. Saleem, M.K. Ravva, F. Cruciani, Z. Kan, J. Wolf, M.R. Hansen, P.M. Beaujuge, J.L. Brédas, *Adv. Mater.* (2016) 8197–8205.
- [16] H. Bellanger, T. Darmanin, E. Taffin De Givenchy, F. Guittard, *RSC Adv.* 2 (2012) 10899–10906.
- [17] U.S. Waware, M. Rashid, A.M.S. Hamouda, *Ionics (Kiel)*. 25 (2019) 1057–1065.
- [18] K.Y. Huang, C.L. Shiu, Y.A. Su, C.C. Yang, J.M. Yeh, Y. Wei, K.R. Lee, *J. Memb. Sci.* 339 (2009) 171–176.
- [19] P.K. Kahol, V. Pendse, N.J. Pinto, M. Traore, W.T.K. Stevenson, B.J. McCormick, J.N. Gundersen, *Phys. Rev. B* 50 (1994) 2809–2814.
- [20] C.C. Han, H.Y. Chen, *Macromolecules* 40 (2007) 8969–8973.
- [21] Y. Şahin, S. Perçin, M. Şahin, G. Özkan, *J. Appl. Polym. Sci.* 91 (2004) 2302–2312.
- [22] A.L. Sharma, R. Singhal, A. Kumar, K.K. Pande, B.D. Malhotra, *J. Appl. Polym. Sci.* 91 (2004) 3999–4006.
- [23] A.L. Sharma, V. Saxena, S. Annapoorni, B.D. Malhotra, *J. Appl. Polym. Sci.* 81 (2001) 1460–1466.
- [24] P.S. Vijayanand, J. Vivekanandan, A. Mahudeswaran, R. Jayaprakasam, *Macromol. Symp.* 362 (2016) 65–72.
- [25] J. Vivekanandan, A. Mahudeswaran, A. Jeeva, P.S. Vijayanand, *J. Polym. Mater.* 31 (2014) 463–475.

- [26] A. Cihaner, A.M. Önal, *Polym. Int.* 51 (2002) 680–686.
- [27] A.L. Sharma, S. Annapoorni, B.D. Malhotra, *Curr. Appl. Phys.* 3 (2003) 239–245.
- [28] Y. Li, Y. Wang, J. Zhang, C. Sun, *Environ. Monit. Assess.* 184 (2012) 4345–4353.
- [29] J.C. LaCroix, A.F. Diaz, *J. Electrochem. Soc.* 135 (1988) 1457–1463.
- [30] P. Yang, M. Yuan, D.F. Zeigler, S.E. Watkins, J.A. Lee, C.K. Luscombe, *J. Mater. Chem. C* 2 (2014) 3278–3284.
- [31] F. Babudri, G.M. Farinola, F. Naso, R. Ragni, *Chem. Commun.* (2007) 1003–1022.
- [32] Y. Zhang, S.C. Chien, K.S. Chen, H.L. Yip, Y. Sun, J.A. Davies, F.C. Chen, A.K.Y. Jen, *Chem. Commun.* 47 (2011) 11026–11028.
- [33] H. Zhou, L. Yang, A.C. Stuart, S.C. Price, S. Liu, W. You, *Angew. Chemie - Int. Ed.* 50 (2011) 2995–2998.
- [34] J. Arias-Pardilla, H.J. Salavagione, C. Barbero, E. Morallón, J.L. Vázquez, *Eur. Polym. J.* 42 (2006) 1521–1532.
- [35] M.A. Cotarelo, F. Montilla, F. Huerta, *Synth. Met.* 158 (2008) 815–820.
- [36] M.S. Wu, T.C. Wen, A. Gopalan, *J. Electrochem. Soc.* 148 (2001).
- [37] H.S.O. Chan, S.C. Ng, W.S. Sim, K.L. Tan, B.T.G. Tan, *Macromolecules* 25 (1992) 6029–6034.
- [38] B.C. Beard, R.A. Brizzolara, *Surf. Sci. Spectra* 2 (1993) 85–88.
- [39] S. Golczak, A. Kanciurzevska, M. Fahlman, K. Langer, J.J. Langer, *Solid State Ionics* 179 (2008) 2234–2239.

- [40] S.N. Kumar, G. Bouyssoux, F. Gaillard, *Surf. Interface Anal.* 15 (1990) 531–536.
- [41] C. Sleight, A.P. Pijpers, A. Jaspers, B. Coussens, R.J. Meier, *J. Electron Spectros. Relat. Phenomena* 77 (1996) 41–57.
- [42] Z. Morávková, E. Dmitrieva, *J. Raman Spectrosc.* 48 (2017) 1229–1234.
- [43] E.M. Geniès, M. Lapkowski, J.F. Penneau, *J. Electroanal. Chem. Interfacial Electrochem.* 249 (1988) 97–107.
- [44] J.M.G. Cowie, in: *Altern. Copolym.*, Springer US, 1985, pp. 1–18.
- [45] F.R. Mayo, F.M. Lewis, *J. Am. Chem. Soc.* 66 (1944) 1594–1601.
- [46] W.S. Huang, A.G. MacDiarmid, *Polymer (Guildf)*. 34 (1993) 1833–1845.
- [47] A. Malinauskas, R. Holze, *J. Appl. Polym. Sci.* 73 (1999) 287–294.
- [48] W.S. Huang, A.G. MacDiarmid, *Polymer (Guildf)*. 34 (1993) 1833–1845.
- [49] M.A. Cotarelo, F. Huerta, C. Quijada, R. Mallavia, J.L. Vázquez, *J. Electrochem. Soc.* 153 (2006).
- [50] S. Padmapriya, S. Harinipriya, K. Jaidev, V. Sudha, D. Kumar, S. Pal, *Int. J. Energy Res.* 42 (2018) 1196–1209.

Declaration of interests

Electrochemical Synthesis of Fluorinated Polyanilines

Nesrine Saidani, Emilia Morallón, Francisco Huerta, Salma Besbes-Hentati, Francisco Montilla

☒ The authors declare that they have no known competing financial interests or personal relationships that could have appeared to influence the work reported in this paper.

☐ The authors declare the following financial interests/personal relationships which may be considered as potential competing interests: